Supporting Information

An asymmetric wettable composite wound dressing prepared by electrospinning with bio-inspired micropatterning enhances diabetic wound healing

Bangrui Yu †, *Chenhui He* †, *Weibin Wang* †, *Yafeng Ren* †, *Jianmin Yang* †,⊥,*, *Shaobin Guo* †,⊥, *Yunquan Zheng* ⊥ *and Xianai Shi* †,⊥,*

† College of Biological Science and Engineering, Fuzhou University, No. 2 Xueyuan Road, Fuzhou 350108, China; ⊥ Fujian Key Lab of Medical Instrument and Biopharmaceutical Technology, Fuzhou University, No. 2 Xueyuan Road, Fuzhou 350108, China

* Correspondence author. E-mail address: jmyang@fzu.edu.cn (J. Yang), shixa@fzu.edu.cn (X. Shi).

MATERIALS AND METHODS

Materials. Poly(ε-caprolactone) (PCL, Mw = ~ 80 kDa), gelatin (Type A, from porcine skin, ~ 300 g of bloom), nylon meshes (pore size: 40 μm, 80 μm), collagenase (≥125 CDU/mg), streptozotocin (STZ) were purchased from Sigma-Aldrich (Shanghai, China). Pioglitazone, formic acid, and pyrrolidone hydrochloride were purchased from Maclin (Shanghai, China). Ethanol, acetic acid, dimethyl sulfoxide (DMSO) were obtained from Sinopharm Chemical Reagent Co., Ltd (Shanghai, China). Phosphate buffer solution (PBS), dulbecco's modified eagle medium (DMEM), penicillin, and streptomycin were purchased from Shanghai Yuanpei Biotechnology Co., Ltd (Shanghai, China). All chemicals were used without further purification.

The bacteria strains of *Escherichia coli* (*E. coli*, ATCC-8739), *Staphylococcus aureus* (*S. aureus*, ATCC-14458), and *Pseudomonas aeruginosa* (*P. aeruginosa*, CMCC B 10104) were purchased from Luwei Microbial Sci&Tech Co, Ltd. (Shanghai, China). Human skin fibroblasts (HSF) and human umbilical vein endothelial cells (HUVECs) were obtained from Dingguo Biotechnology Co., Ltd. (Beijing, China). Live/dead cell staining kits and 3-(4,5-dimethylthiazol-2yl)-2,5-diphenyl tetrazolium bromide (MTT) were purchased from BestBio Co., Ltd. (Shanghai, China). Diabetic (*db/db*) mice at six weeks of age, were purchased from Model Animal Research Center of Nanjing University (Nanjing,

China). SD rats with weight of 180-220 g were purchased from Wu's Experimental Animals (Fuzhou, China).

Determination of water vapor transmission rate (WVTR). The WVTR of asymmetric wettable dressings was measured according to the American Society for Testing and Materials (ASTM) standards. Briefly, the sample was cut into a disc shape and installed in the mouth of vial which containing deionized water. Afterward, the vial sealed with sample was placed in an incubator (HCJ-6D, Changzhou, China) at a constant temperature (37 °C) and humidity (79%). The WVTR was calculated as below[1].

$$\mathrm{WVTR} = \frac{\Delta_m/\Delta_t}{A}$$

where "Δ_m/Δ_t" was the weight of moisture loss for 24 h (g/24 h), and "A" was the effective transfer area (m^2).

Evaluation of antibacterial adhesion effect. According to previous work[2,3], the sample (1 cm × 1 cm) was sterilized with UV irradiation for 0.5 h, and then placed on a 24-well plate with the tested surface facing up. Afterward, 1 mL of the bacteria suspension（1×10^6 CFU/mL） was dropped on the surface of the sample, and then incubated for 4 h under 37 °C at static conditions. After removing the bacteria suspension by place the sample vertically for 3 min, the sample was transferred to an Erlenmeyer flask which containing 25 mL of fresh LB medium. After incubation 24 h with a stirring speed of 120 rpm, the sample was rinsed repeatedly with sterile PBS to remove any non-adherent bacteria.

As for quantitative analysis, the sample was transferred to a sterile test tube which containing 5 mL of fresh PBS, and the adhered bacteria were separated by ultrasonic treatment. After diluted with PBS, 100 μL of the bacterial solution was seeded on a solid LB medium plate and incubated for 24 h. Finally, the colonies were counted to calculate the number of adhered bacteria on the surface of sample.

As for SEM observation, the sample was fixed with a 2.5% glutaraldehyde solution for 30 min, and then gradient dehydration with different concentrations of ethanol (25%, 50%, 75%, 95%, 100%). Subsequently, the sample was dried in atmospheric condition, and gold-coating before SEM observation.

Evaluation of biocompatibility and wound healing *in vitro*. HUVECs were cultured in DMEM

medium supplemented with 10% of FBS and 1% of penicillin-streptomycin, and HSF cells were cultured in DMEM medium supplemented with 15% of FBS and 1% of penicillin-streptomycin. The cells were cultured in a 37 °C incubator containing 5% of CO_2. Cells were harvested after reaching 80% confluence and then resuspended in DMEM medium. A volume of 1 mL cell suspension with the cell density of 2×10^4 cells/mL was seeded into each well. Afterward, the dressings were added and co-culture for different times (1 day, 3 days). The cytotoxicity and cell proliferation were measured by MTT assay. The cells were incubated with 1 mL of MTT solution (0.5 mg/mL) for 4 h at 37 ℃. After remove the MTT solution, 1 mL of DMSO was added to dissolve the crystals. And then, 100 μL of the final solution was added to 96-well plates to measure the absorbance intensity at 570 nm. In addition, the cells were stained with a live/dead staining assay kit according to the manufacturer's protocol. The cells in each well were washed twice with PBS, and then 300 μL of live/dead stock solution was added. After incubation 30 min, the cells on the wound dressing were observed with an inverted fluorescence microscope.

To evaluate the effect of asymmetric wettable dressings on HSF and HUVECs migration, an *in vitro* wound healing model was investigated. HSF (2×10^5 cells/well) and HUVECs (4×10^5 cells/well) were seeded into 6-well plates and then cultured until the cells formed a confluent monolayer. Afterward, scrap the monolayer of cells in a straight line using a tip of sterile pipette, and then removed any cell debris with PBS washing. Subsequently, 2 mL of serum-free medium was added to each well, and then a sterilized dressing (2 cm × 2 cm) was added. The cell migration was recorded by a microscope, and the wound closure area was calculated by ImageJ software. The cell migration rate was:

$$\text{Cell migration}\% = \frac{A_0 - A_t}{A_0} \times 100\%$$

Where A_0 was the scratch wound area at 0 h, and A_t was the scratch wound area after cell migration.

Angiogenesis test. Matrigel was thawed at 4 °C overnight. Afterward, 250 μL of Matrigel was added to a precooled 24-well plate, and then incubated 20 min. Subsequently, HUVECs were seeded into each well (2×10^4 cells), and the fresh medium containing different dressings were added. After incubation 6 h, the dressings were taken out to evaluate the angiogenic capacity of HUVECs with a microscope. The tubular structure was quantified with an Image J software.

Development of type 1 diabetic rat model. The SD male rats with a weight of 180–220 g were used to development of type 1 diabetic model. Briefly, acclimating and observing SD rats for one week, and then fasting overnight before inducing diabetes. Afterward, a single intraperitoneal injection of streptozotocin (STZ) (70 mg/kg) was performed on the rat. During the following week, the fasting blood glucose concentration was regularly measured by a blood glucose meter. The model was regarded as successful when the blood glucose concentration was higher than 16.7 mM.

***In vivo* evaluation of diabetic wound healing.** The wounds were photographed at predetermined time points, and the closed wound area was calculated using the ImageJ software. The calculation formula was:

$$\text{closure}\% = \frac{A_0 - A_t}{A_t} \times 100\%$$

Where A_0 was the wound area on day 0, and A_t was the wound area on day t.

Histopathological analysis. The wound tissue used for histological analysis was fixed with 4% paraformaldehyde, dehydrated with gradient ethanol, and then the tissue was embedded in paraffin and cut into 4 mm sections. Histological analysis was performed by hematoxylin and eosin (H&E) staining and Masson's trichrome staining according to the manufacturer's instructions. The stained sections were then observed with an optical microscope. Measurement and quantification of collagen deposition with IPP 6.0 software.

CD31, α-SMA, and Ki67 were immunofluorescently stained according to the manufacturer's protocol in *db/db* mice. Briefly, the tissue sections blocked with BSA were incubated with the corresponding primary antibodies overnight at 4 °C. After washing 5 times with PBS, a secondary antibody labeled with fluorescein was added by dropwise, and the nuclei were stained with DAPI. Quantitative determination of CD31, α-SMA, Ki67 was performed using IPP 6.0 software. In addition, MMP-9 and MMP-2 were immunohistochemically stained according to the manufacturer's protocol. Finally, stained images were captured with a fluorescence microscope. For histological analysis of STZ rats, the same steps as above were taken.

SECTION 1

Model for surface wettability calculation. Wettability is one of the important characteristics of solid surfaces and reflects the behavior of liquids on solid surfaces[4-7]. The wettability of an ideal smooth surface can be described by Young's equation:

$$\cos\theta = {(\gamma_{sv} - \gamma_{sl})}/{\gamma_{lv}} \quad \text{S1}$$

Where γ_{sv}, γ_{sl} and γ_{lv} were the surface tension between the solid-vapour, solid-liquid, and liquid-vapour contact surfaces, $\cos\theta$ was the intrinsic contact angle of the solid surface.

For the micropatterned biomimetic hydrophobic surface, the space between the liquid and rough surface is filled with air, and the liquid cannot completely contact with the surface. Therefore, the liquids on the biomimetic hydrophobic surface can be described by Cassi Baxter model, and the contact angle formula as below:

$$\cos\theta_A = f_1\cos\theta_1 - f_2 \quad \text{S2}$$

Where θ_A was the apparent contact angle, f_1 was the ratio of solid material to liquid contact, θ_1 was the contact angle of ideal solid material, and f_2 wass the ratio of air to liquid contact ($f_1 + f_2 = 1$). In our work, the outer layer was PCL which a hydrophobic material. Therefore, the $90° < \theta_1 < 180°$, and $-1 < \cos\theta_1 < 0$, thus $\theta_A > \theta_1$. Hence, the biomimetic hydrophobic layer showing higher hydrophobic properties.

The enhanced hydrophilic properties of gelatin nanofiber membranes can be explained by the Wenzel model. The formula for the contact angle of hydrophilic surfaces was:

$$\cos\theta_B = r\cos\theta_2 \quad \text{S3}$$

Where θ_B was the apparent contact angle, r was the ratio of the actual area to the projected area ($r \geq 1$), and θ_2 was the contact angle of the ideal solid material. Since the gelatin has hydrophilic properties, and

thus the $0° < \theta_2 < 90°$, $0 < \cos\theta_2 < 1$, $\theta_B < \theta_2$. Therefore, the surface of the gelatin nanofiber membrane shows a more hydrophilic property.

REFERENCES

1. Hu, S.; Cai, X.; Qu, X.; Yu, B.; Yan, C.; Yang, J.; Li, F.; Zheng, Y.; Shi, X. Preparation of biocompatible wound dressings with long-term antimicrobial activity through covalent bonding of antibiotic agents to natural polymers. *Int. J. Biol. macromol.* **2019**, *123*, 1320-1330.

2. Hu, J.; Lin, J.; Zhang, Y.; Lin, Z.; Qiao, Z.; Liu, Z.; Yang, W.; Liu, X.; Dong, M.; Guo, Z. A new anti-biofilm strategy of enabling arbitrary surfaces of materials and devices with robust bacterial anti-adhesion via a spraying modified microsphere method. *J. Mater. Chem. A* **2019**, *7*, 26039-26052.

3. Sivakumar, P. M.; Prabhawathi, V.; Neelakandan, R.; Doble, M. Chalcone coating on cotton cloth–an approach to reduce attachment of live microbes. *Biomater. Sci.* **2014**, *2*, 990-995.

4. Nakajima, A. Design of hydrophobic surfaces for liquid droplet control. *NPG Asia Mater.* **2011**, *3* (5), 49.

5. Wenzel, R. N. Resistance of solid surfaces to wetting by water. *Ind. Eng. Chem.* **1936**, *28*, 988-994.

6. Cassie, A.; Baxter, S. Wettability of porous surfaces. *Trans. Faraday Soc.* **1944**, *40*, 546-551.

7. Zhang, X.; Wang, L.; Levänen, E. Superhydrophobic surfaces for the reduction of bacterial adhesion. *RSC Adv.* **2013**, *3*, 12003-12020.

SECTION 2

SUPPORTING FIGURES

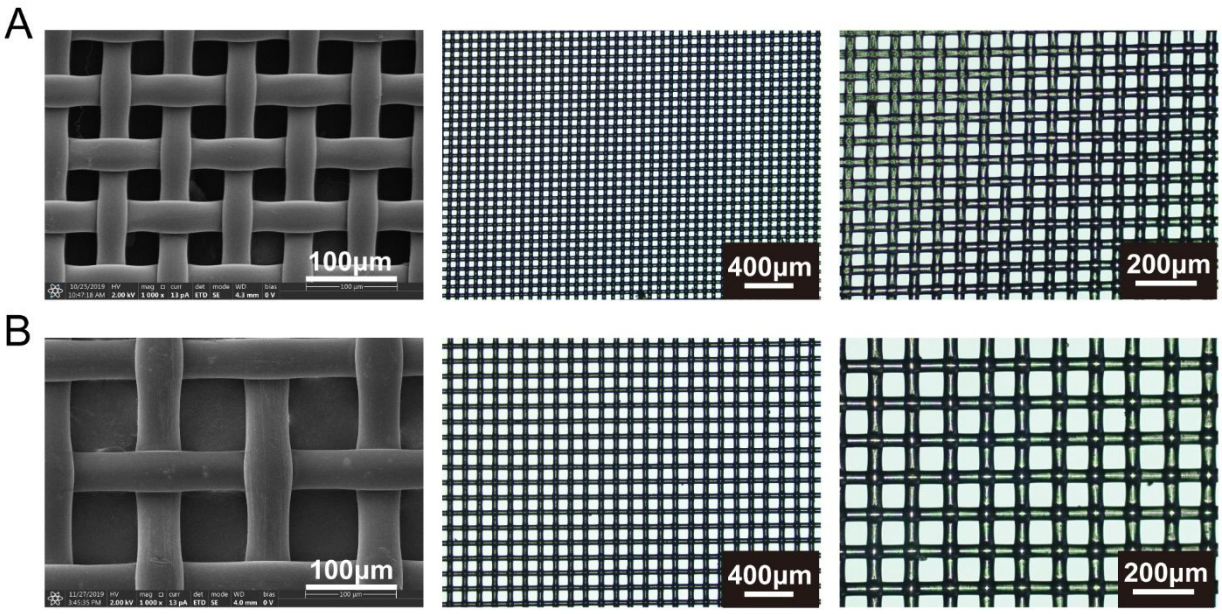

Figure S1. SEM and optical microscope images of nylon meshes with pore size of (A) 40 µm and (B) 80 µm.

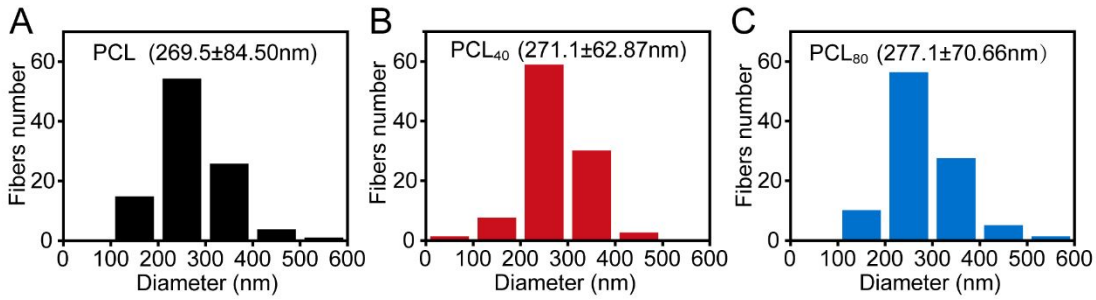

Figure S2. Nanofiber diameter distribution of (A) PCL, (B) PCL_{40}, and (C) PCL_{80} membrane.

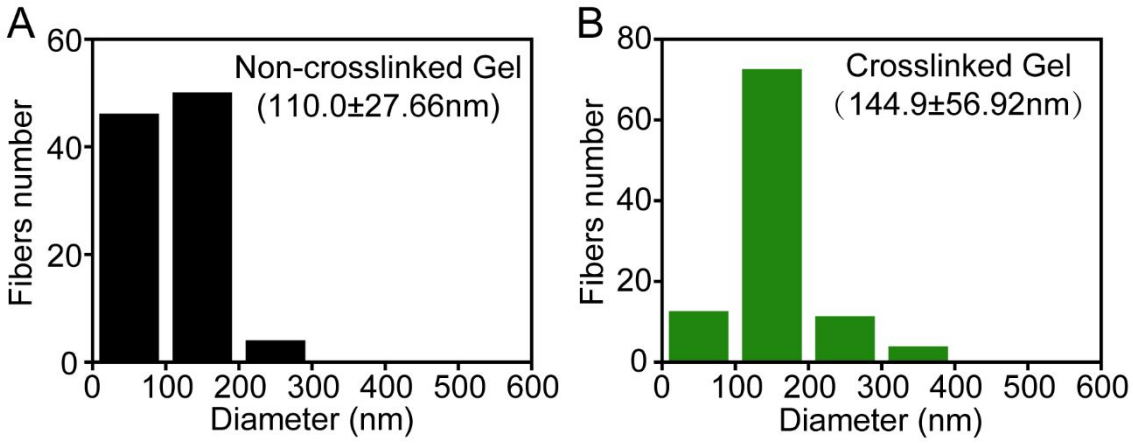

Figure S3. Diameter distribution of gelatin nanofibers before and after crosslinking reaction. (A) Non-crosslinked Gel and (B) crosslinked Gel.

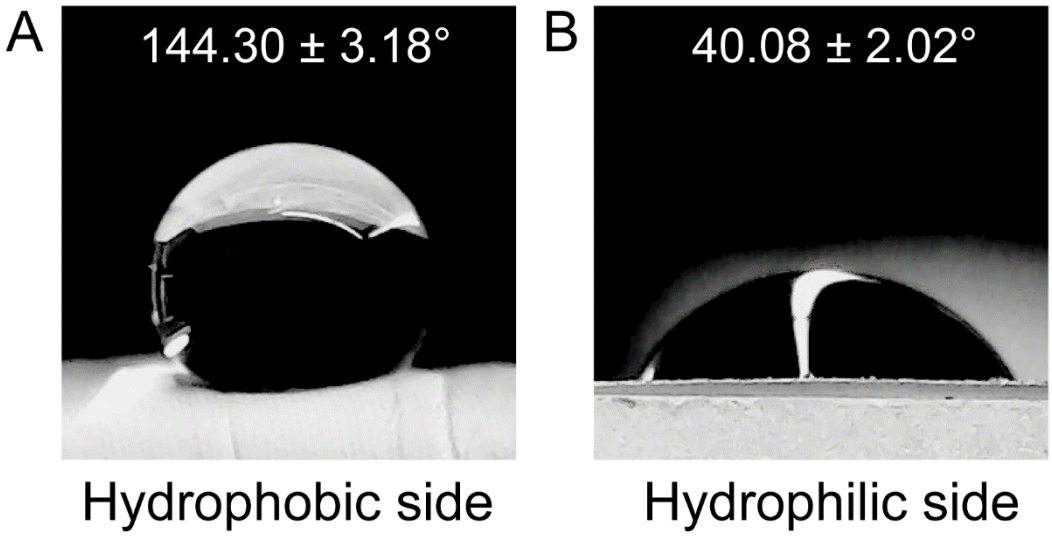

Figure S4. WCA images of the asymmetric wettable composite wound dressing (PCL_{40}/Gel).

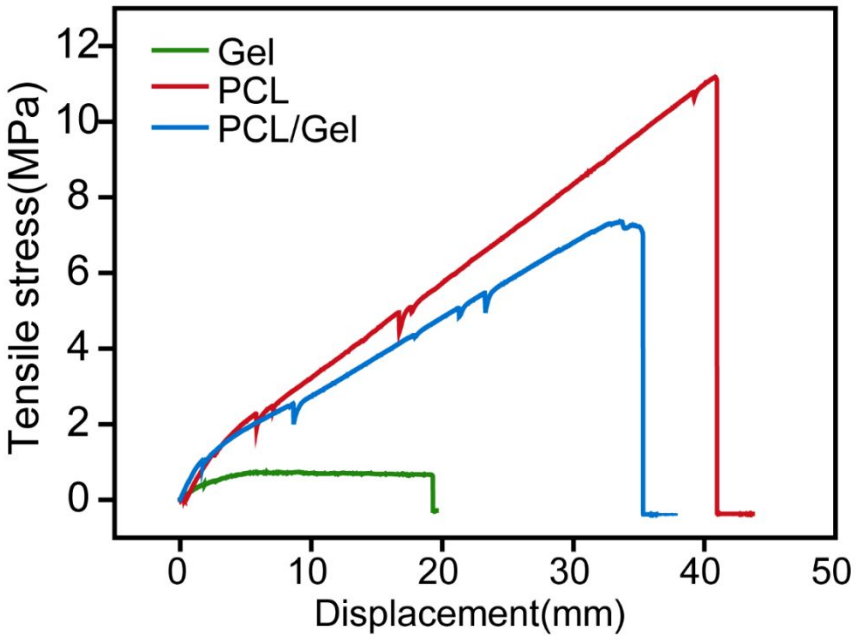

Figure S5. Stress-displacement curves of PCL, Gel, PCL/Gel.

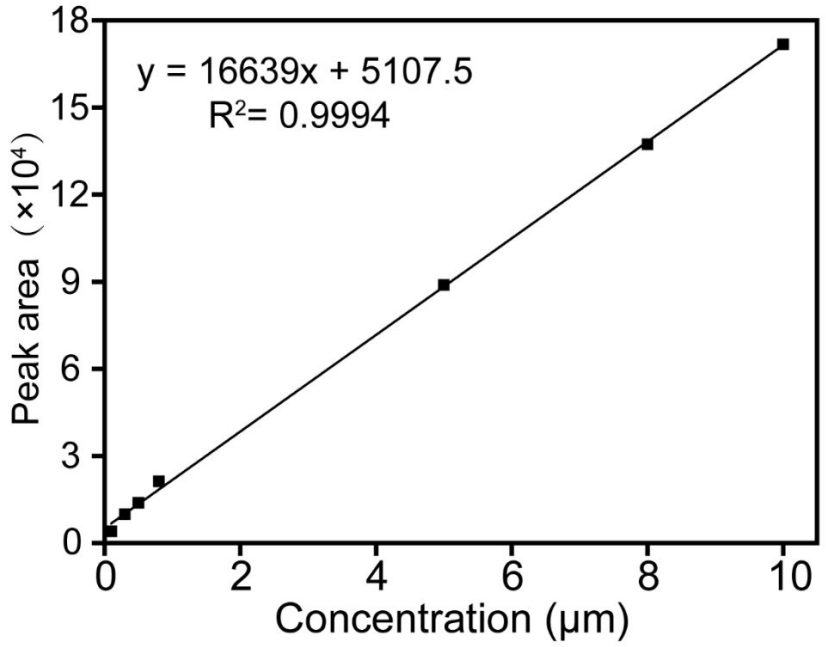

Figure S6. Standard curve of pioglitazone with different concentrations in HPLC.

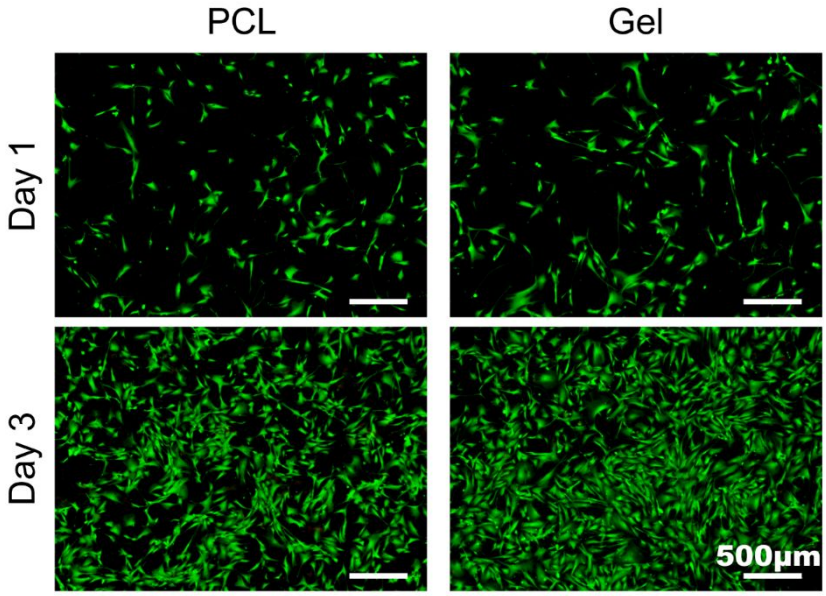

Figure S7. Live/dead staining images of HSF cells cultured in medium containing PCL or Gel nanofibers.

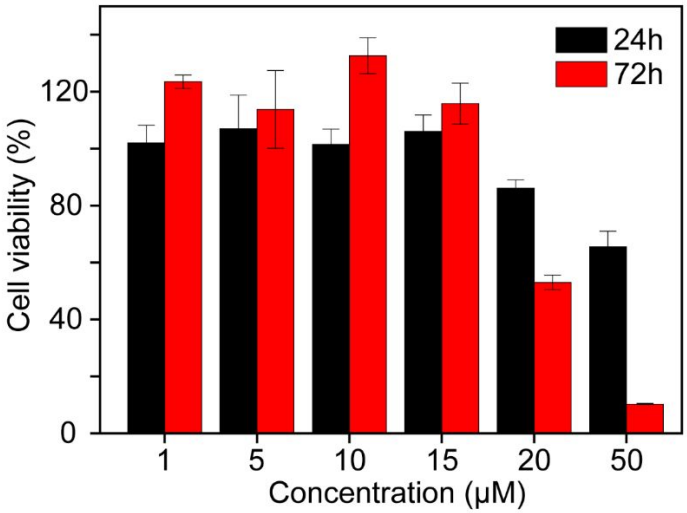

Figure S8. Cell viability of HSF in different concentrations of piroglitazone at different culture times by MTT assay.

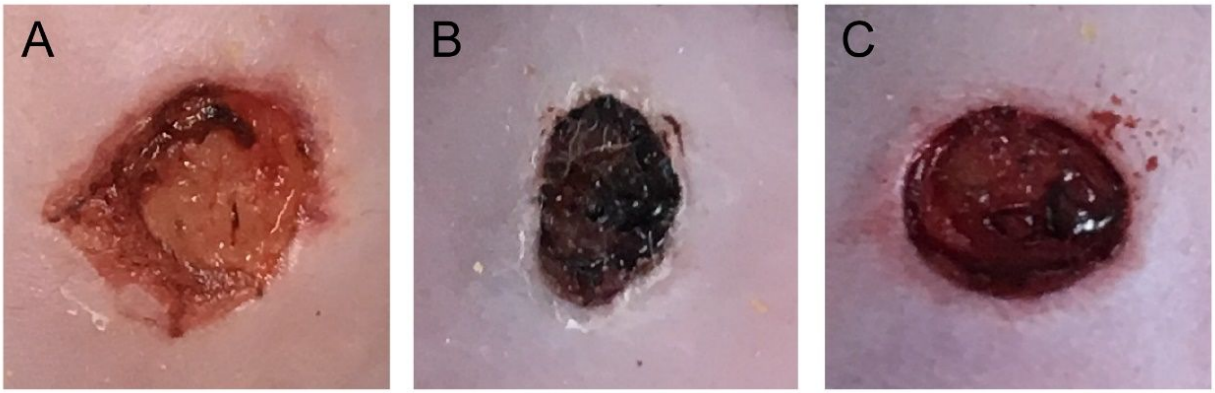

Figure S9. Photographs of abnormal wound healing in the control group at day 7 in *db/db* mice. (A) Inflamed wound, (B) crusted wound, and (C) the bleeding wound.

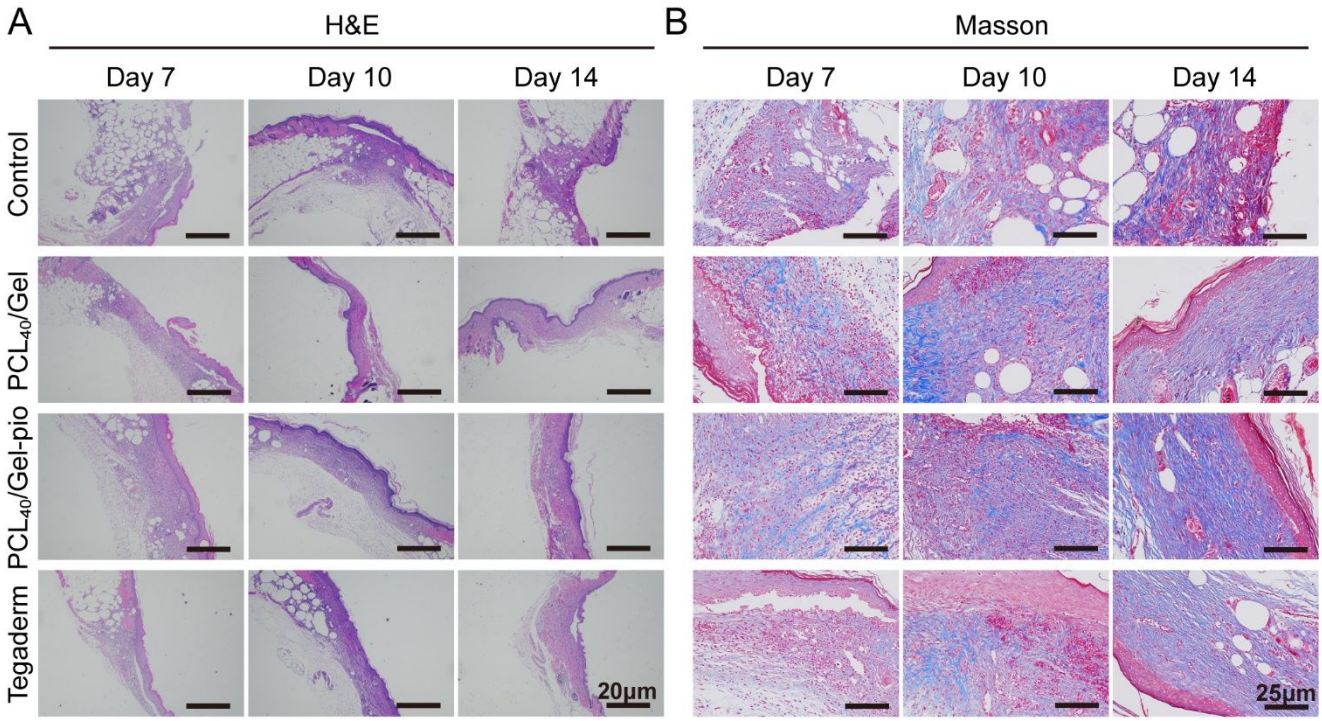

Figure S10. Representative photographs of the immunohistochemical staining at different times. (A) H&E staining and (B) Masson's trichrome staining.

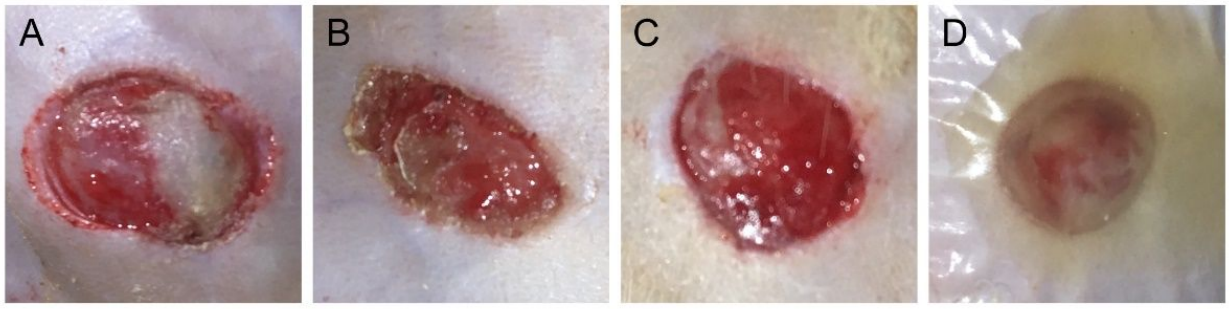

Figure S11. Photographs of abnormal wound healing on day 5 in STZ rats. (A) Inflamed wounds, (B) crusted wounds, and (C) bleeding wounds in the control group. (D) Wound exudate accumulated under the dressing in the Tegaderm group.

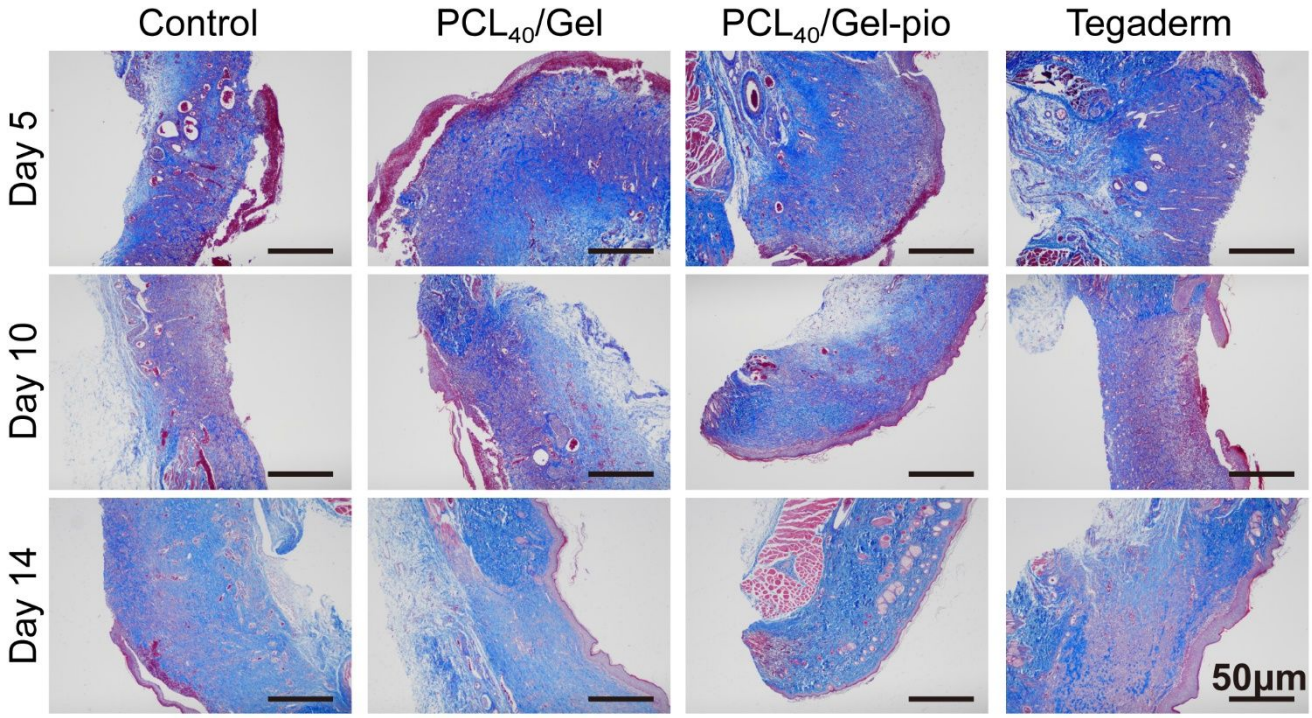

Figure S12. Representative photographs of the Masson's trichrome staining on day 5, day 10, and day 14.

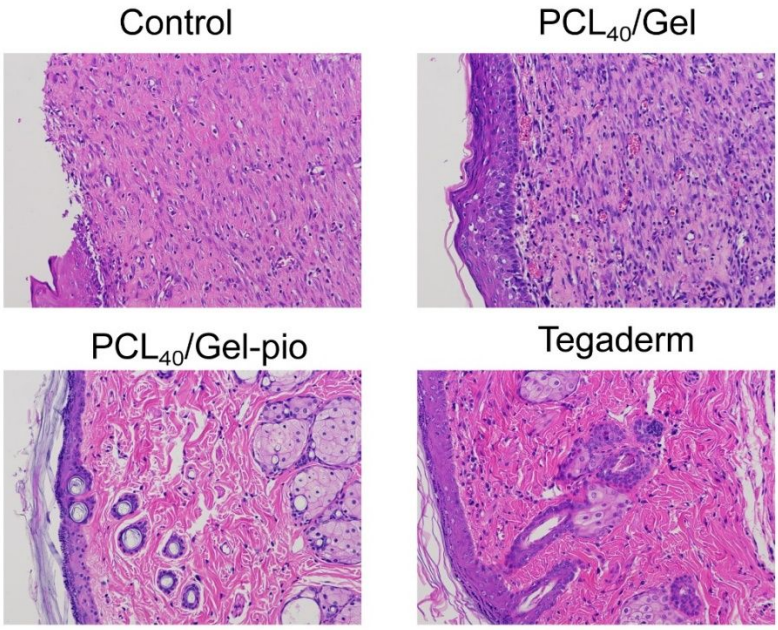

Figure S13. Representative photographs of the H&E staining on day 21.

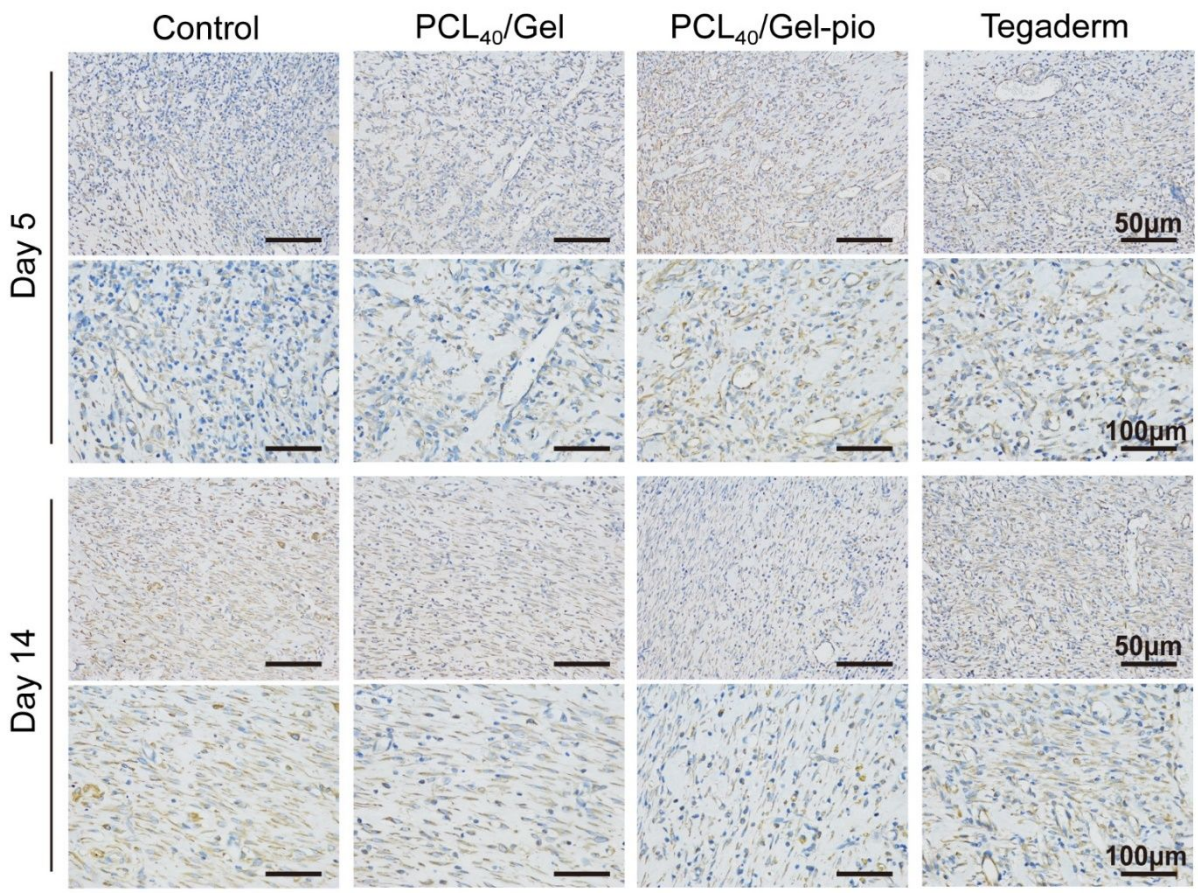

Figure S14. Representative photographs of the VEGF immunochemistry staining on day 5 and day 14.